Rapid glacier retreat rates observed in West Antarctica

Authors: P.Milillo[1,2,4*], E.Rignot[2,3,5], P.Rizzoli[4], B.Scheuchl[2], J.Mouginot[2,6] , J.L. Bueso-Bello[4], P.Prats-Iraola[4], L.Dini[7]

Affiliations:

[1] Department of Civil & Environmental Engineering, University of Houston, TX, USA

[2] Department of Earth System Science, University of California, Irvine, CA, USA

[3] Department of Civil & Environmental Engineering, University of California, Irvine, CA, USA

[4] German Aerospace Center (DLR), Microwaves and Radar Institute, Munich, Germany

[5] Jet Propulsion Laboratory, California Institute of Technology, Pasadena, CA, USA

[6] Univ. Grenoble Alpes, CNRS, IRD, Grenoble INP, IGE, 38000, Grenoble, France

[7]Italian Space Agency (ASI), Matera, Italy

Supplementary Material

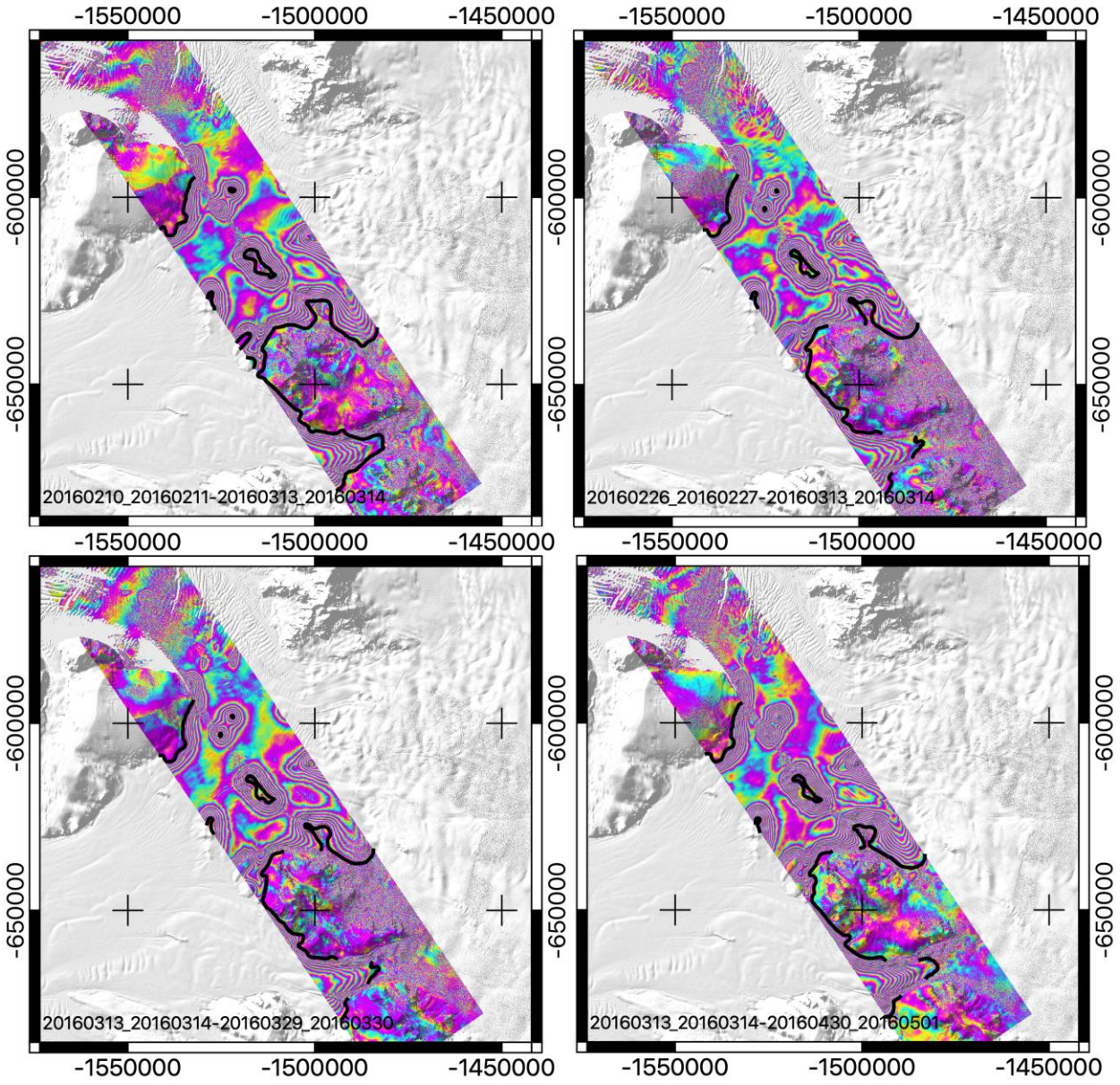
-1550000
-1500000
-1450000
-600000
-650000
20160210_20160211-20160313_20160314
20160226_20160227-20160313_20160314
20160313_20160314-20160329_20160330
20160313_20160314-20160430_20160501

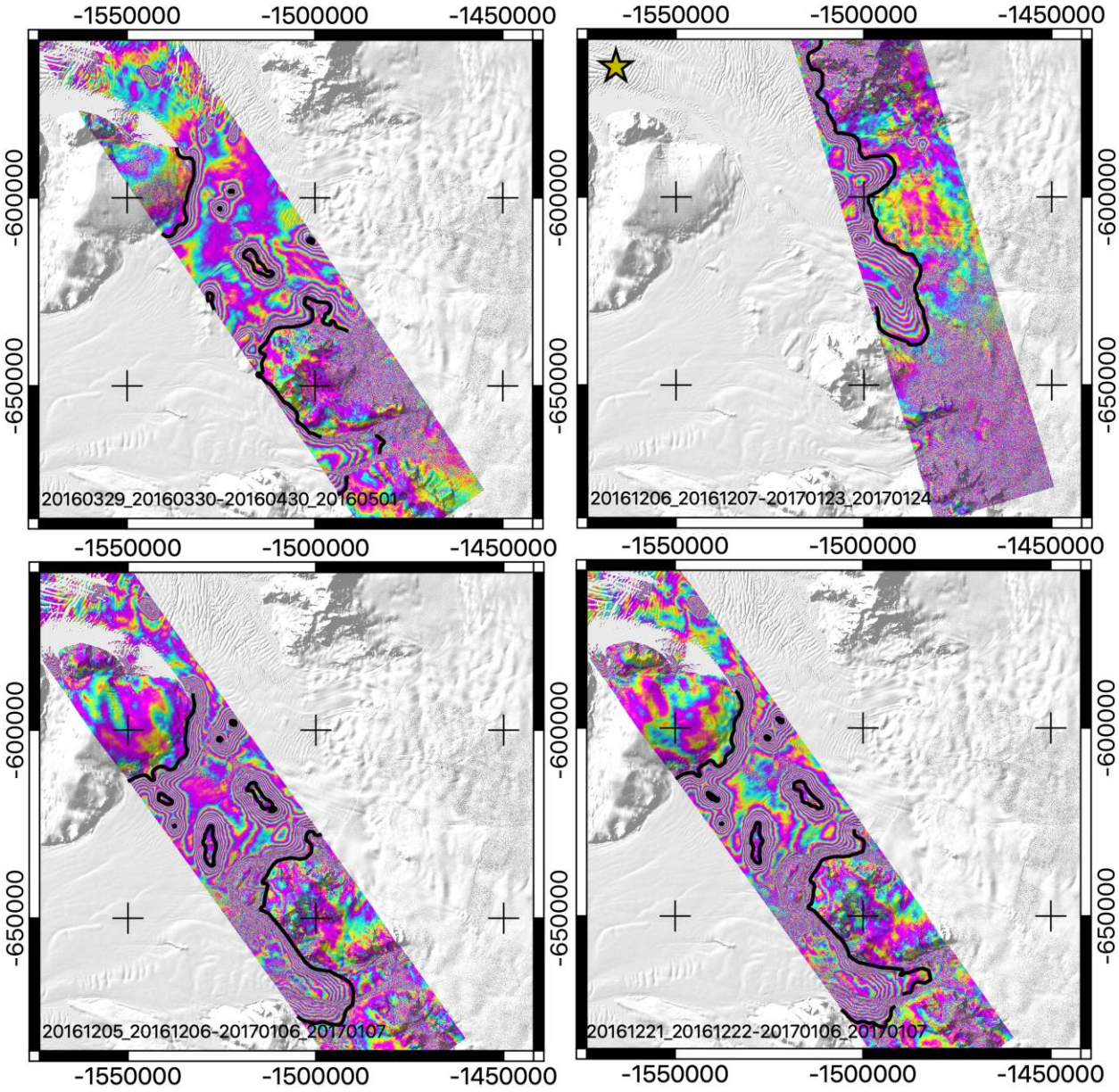
-1550000
-1500000
-1450000
-600000
-650000
20160329_20160330-20160430_20160501
20161206_20161207-20170123_20170124
20161205_20161206-20170106_20170107
20161221_20161222-20170106_20170107

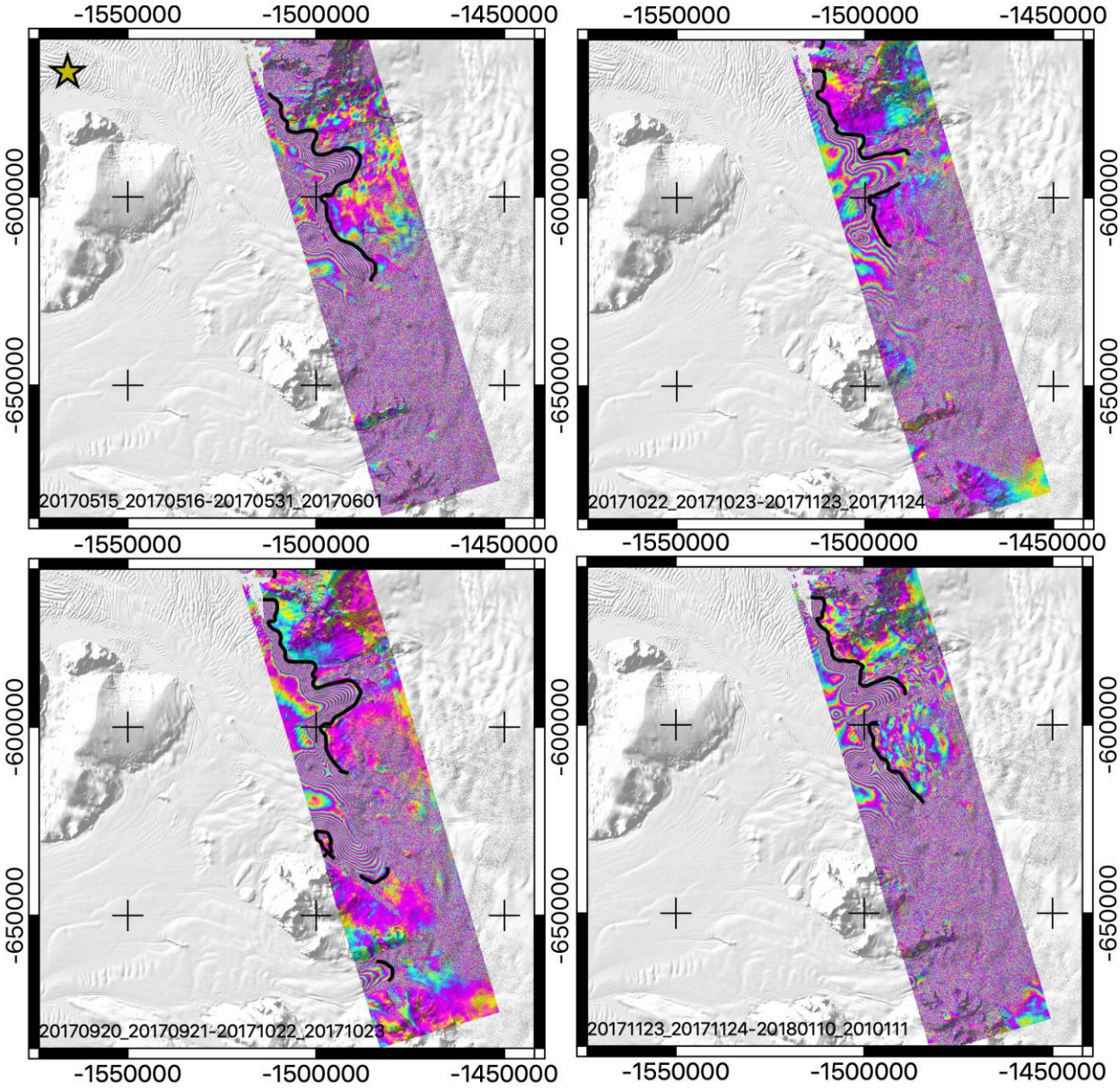
-1550000
-1500000
-1450000
-600000
-650000
20170515_20170516-20170531_20170601
20171022_20171023-20171123_20171124
20170920_20170921-20171022_20171023
20171123_20171124-20180110_2010111

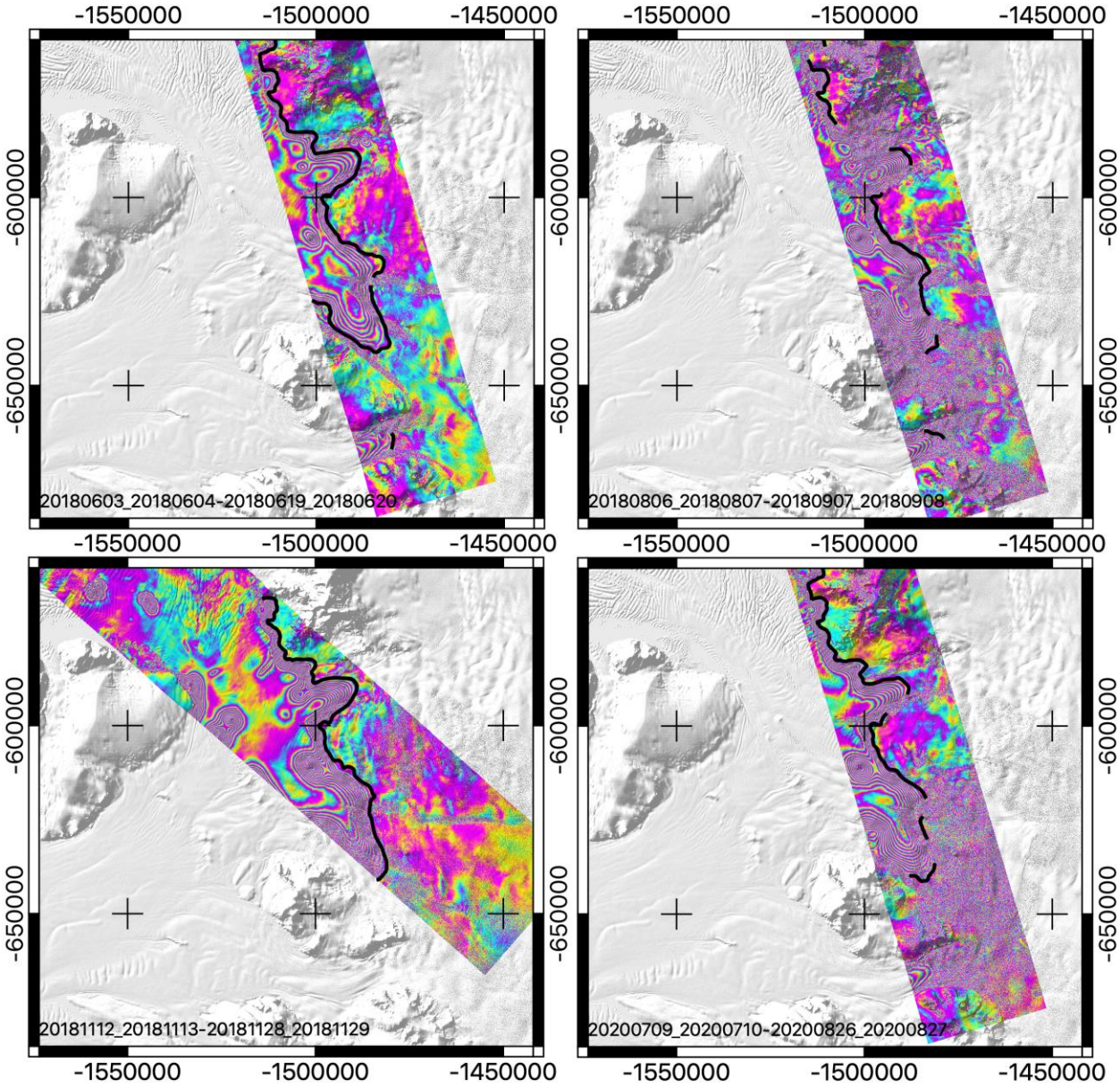
-1550000
-1500000
-1450000
-600000
-650000
20180603_20180604-20180619_20180620
20180806_20180807-20180907_20180908
20181112_20181113-20181128_20181129
20200709_20200710-20200826_20200827

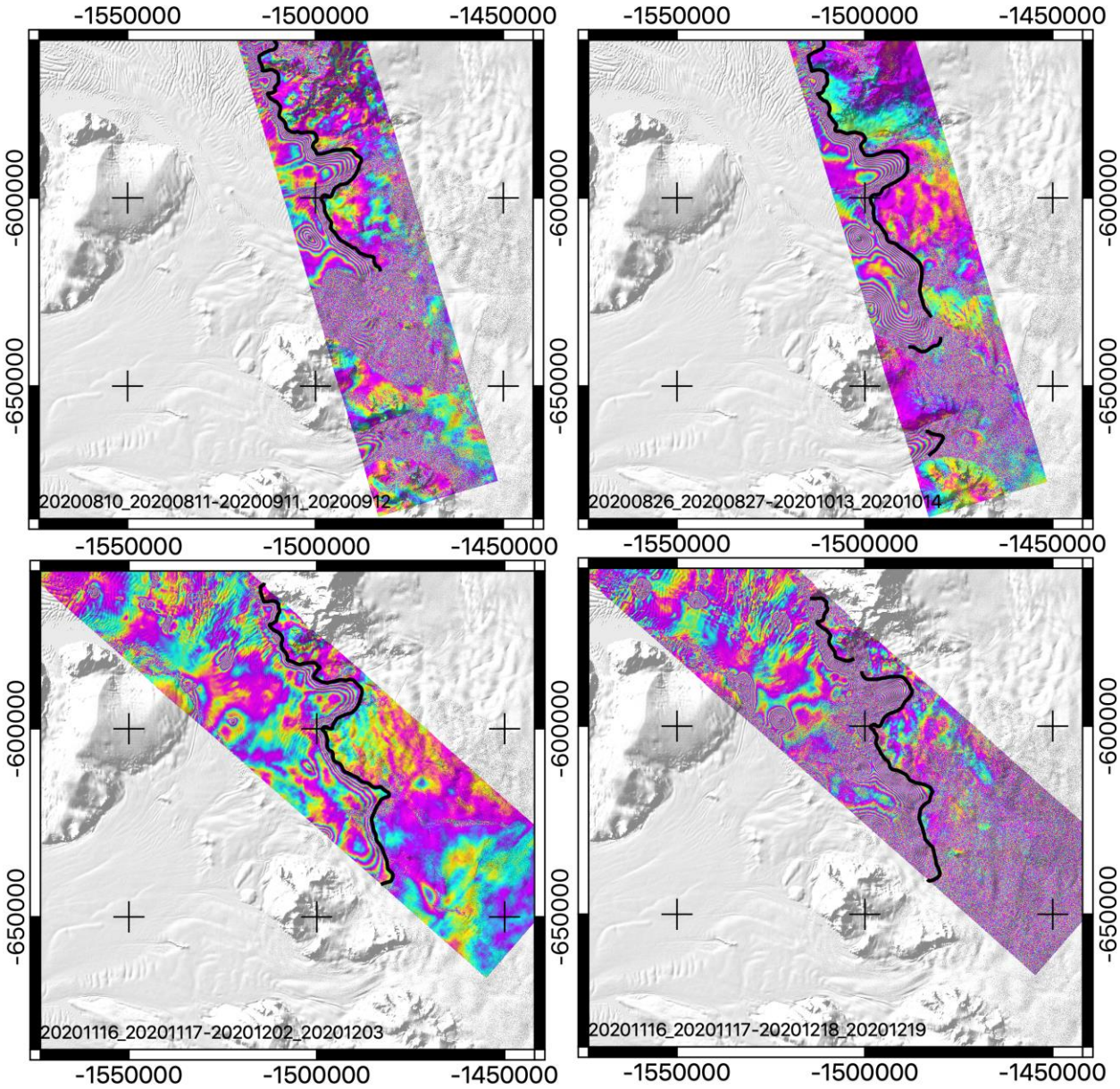
-1550000
-1500000
-1450000
-600000
-650000
20200810_20200811-20200911_20200912
20200826_20200827-20201013_20201014
20201116_20201117-20201202_20201203
20201116_20201117-20201218_20201219

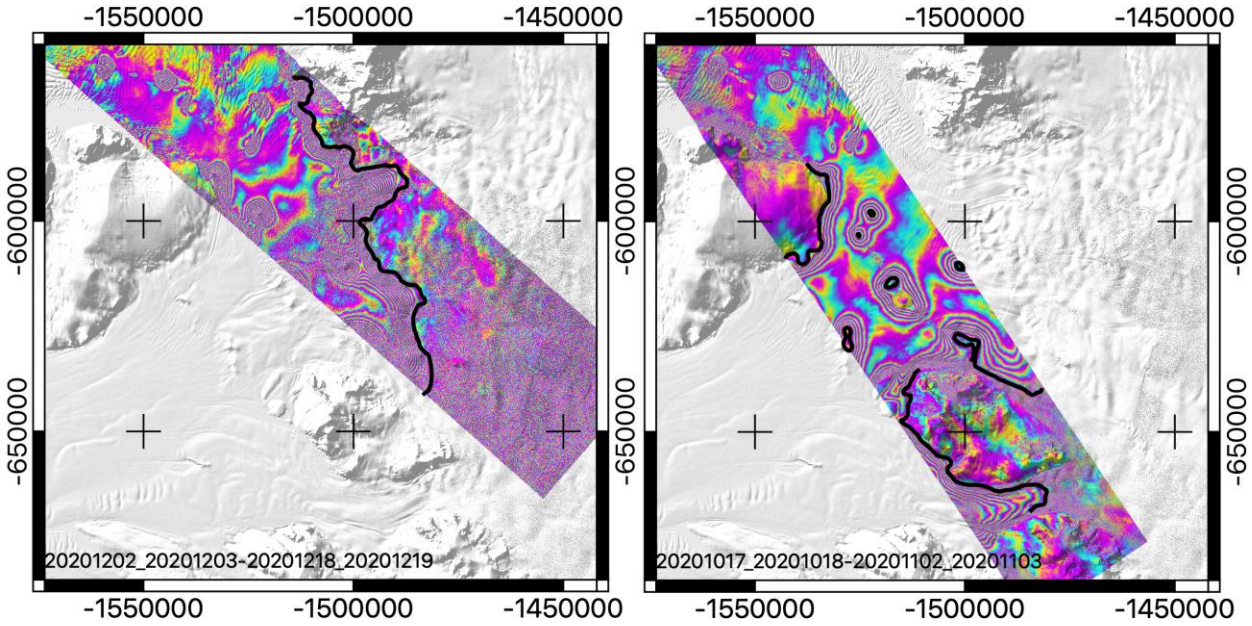

Figure S1. CSK DInSAR data over the Pope, Smith and Kohler Glaciers, West Antarctica from 2016 to 2020. Each fringe, or 360-degree cycle in phase, corresponds to a relative displacement of the ice surface of 15 mm in the line of sight of the radar, or 17 mm in the vertical direction. Dates are reference image year, month, and day minus registered image year, month and day. Grounding line positions delineated for each DInSAR interferogram are shown in black. Backgound image is a MODIS image of Antarctica. Yellow star at the top left indicates double difference interferograms 5 months apart showing the abrupt retreat of Pope Glacier.

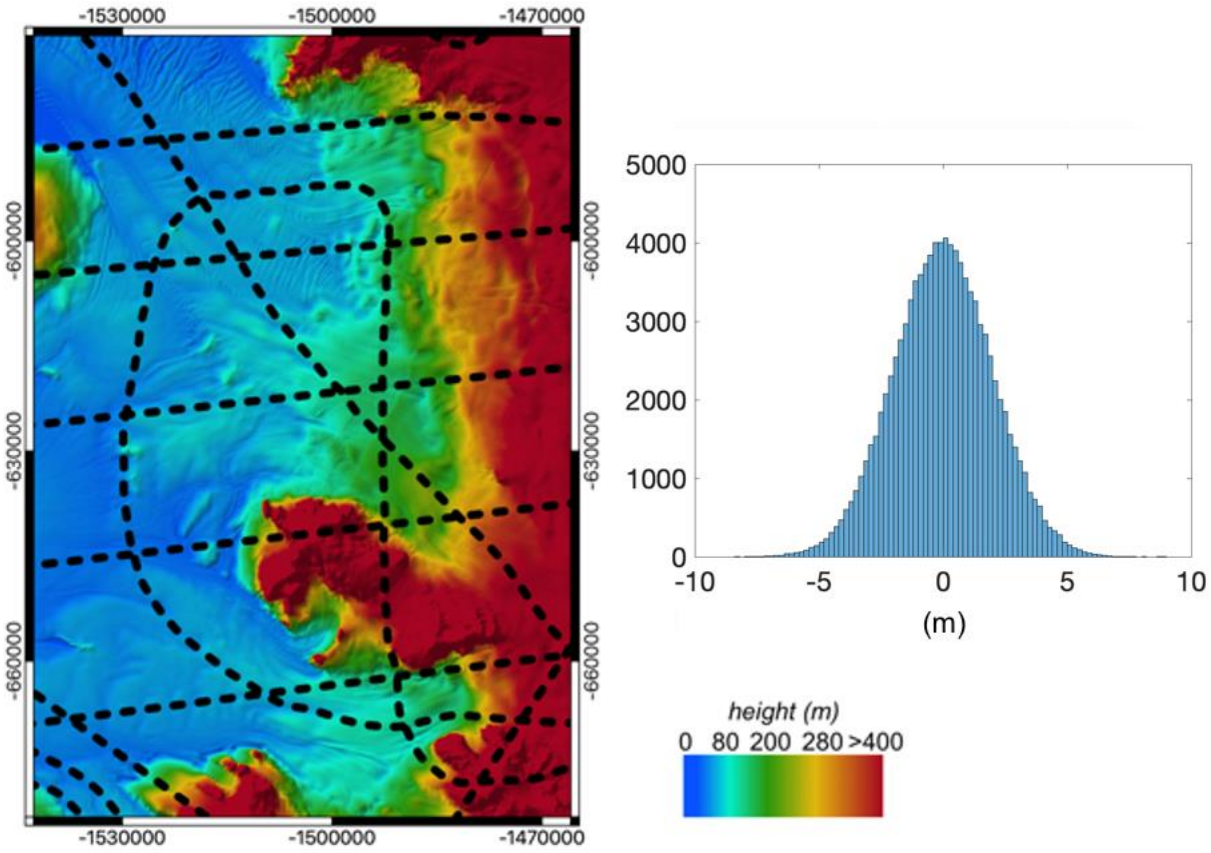

Figure S2. Distribution of height differences between the NASA Airborne Topographic Mapper (ATM) laser altimetry surface elevation data minus the surface elevation from the TanDEM-X over Kohler, Smith and Pope glaciers, West Antarctica, in meters, along the tracks shown as dotted black lines on the left panel. Standard Deviation is 2.1 meters.

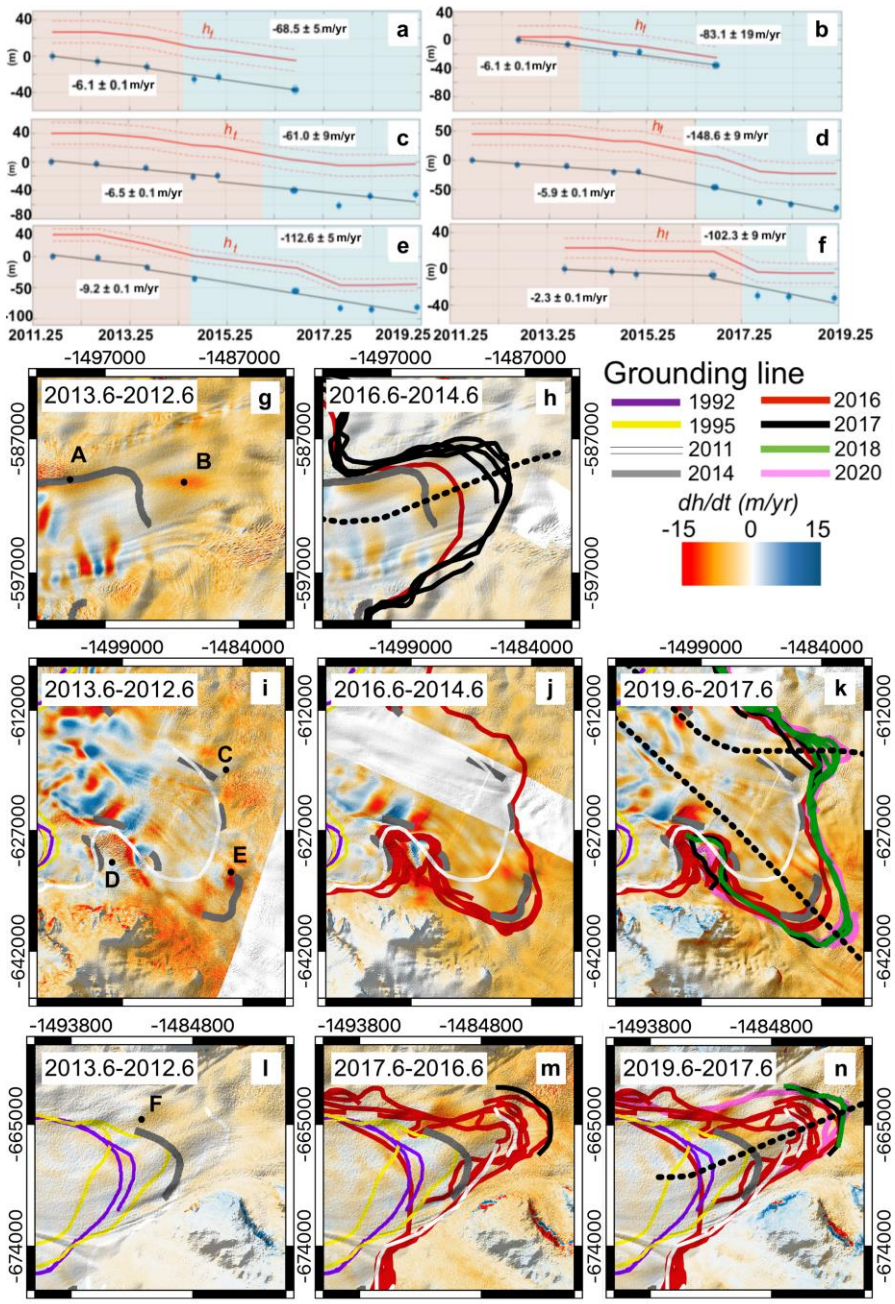

Figure S3. Rapid changes in ice thickness, dH_i/dt, of Pope, Smith East and West, and Kohler glaciers from TDX data (blue dots) for the time period 2011–2019 over grounded ice (red domain, $dh/dt_{gd} = dH_i/dt$) at locations A - F, with height above flotation, h_f (red) with 1σ uncertainty (dashed red), converted into a change in ice thickness, dH/dt, over floating ice (blue domain) in meters per year. Map of changes in ice surface elevation, dh/dt, *for* (**g**-**h**) Pope, (**j**-**l**) Smith East and West and (**n**-**p**) Kohler glaciers in meters per year with grounding line color coded by years.

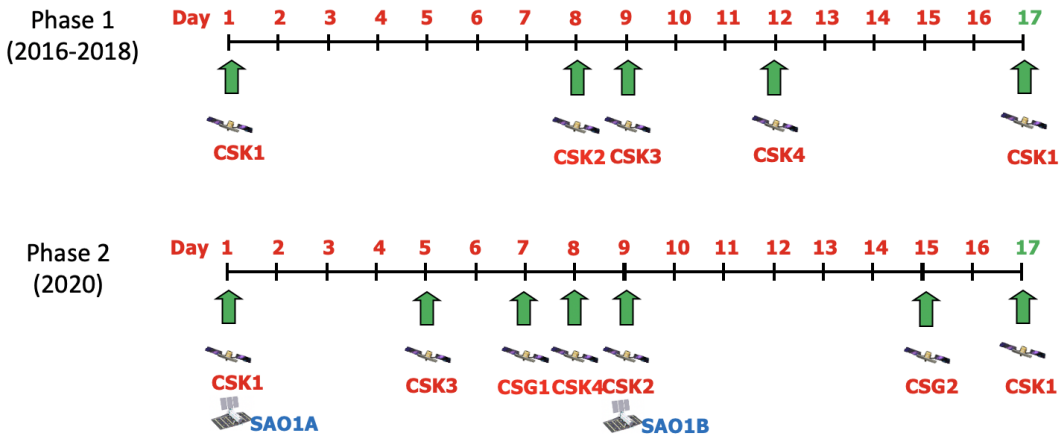

Figure S4. Satellite acquisition schedule planned for this study. CSK2 and CSK3 data are used in Phase 1 of this study. CSK4-CSK2 data are used for phase 2 of this study.

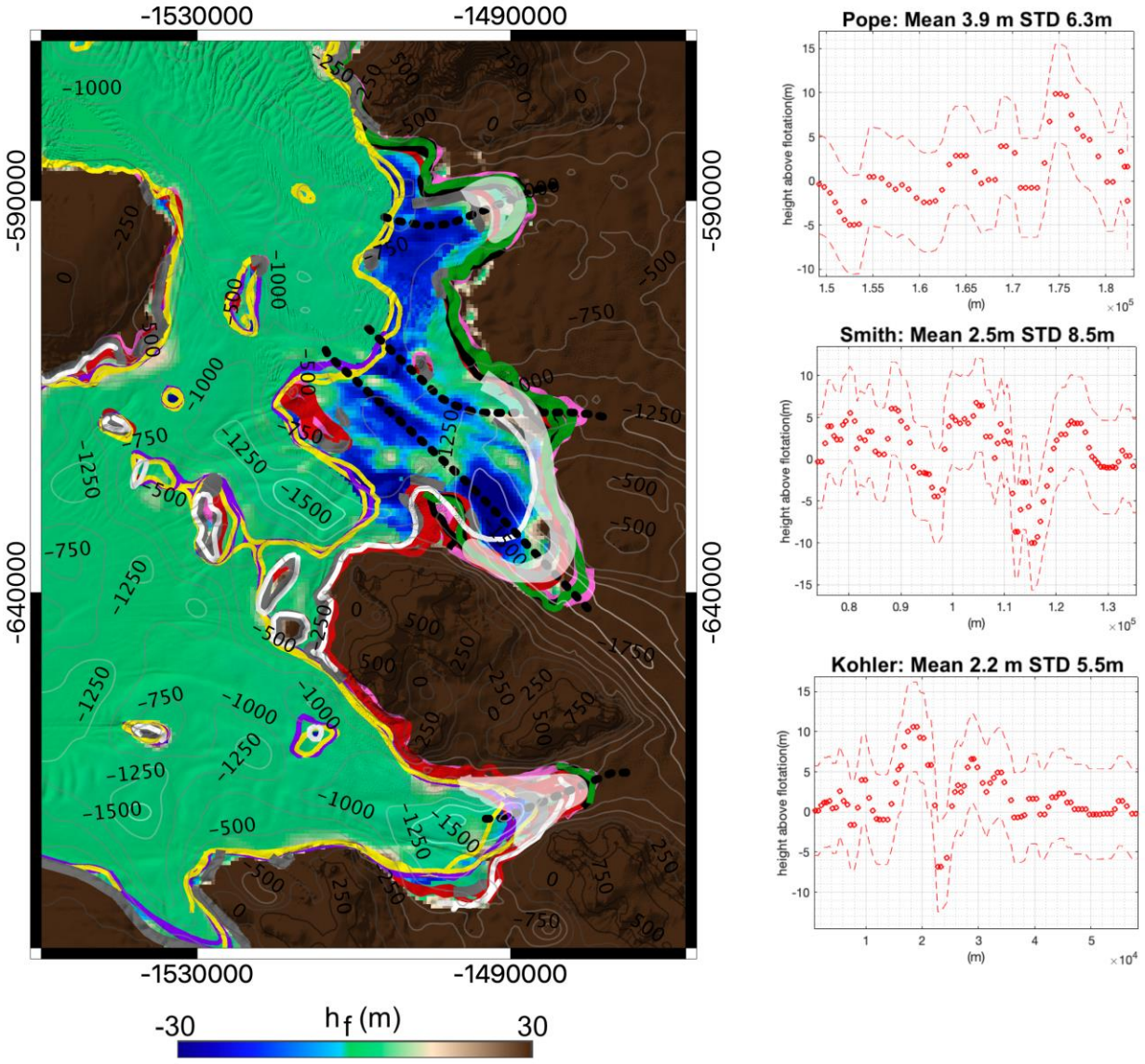

Figure S5. (Left) Height above flotation, h_f, as calculated in Eq. 2 from BedMachine Antarctica version 2020_06_18. (Right) Profiles of average height above flotation, h_f, calculated across the grounding zones of the three major glaciers (Pope, Smith East/West, and Kohler) highlighted as transparent white boxes in the left panel. 500-m contour levels indicating bed elevation (grey)

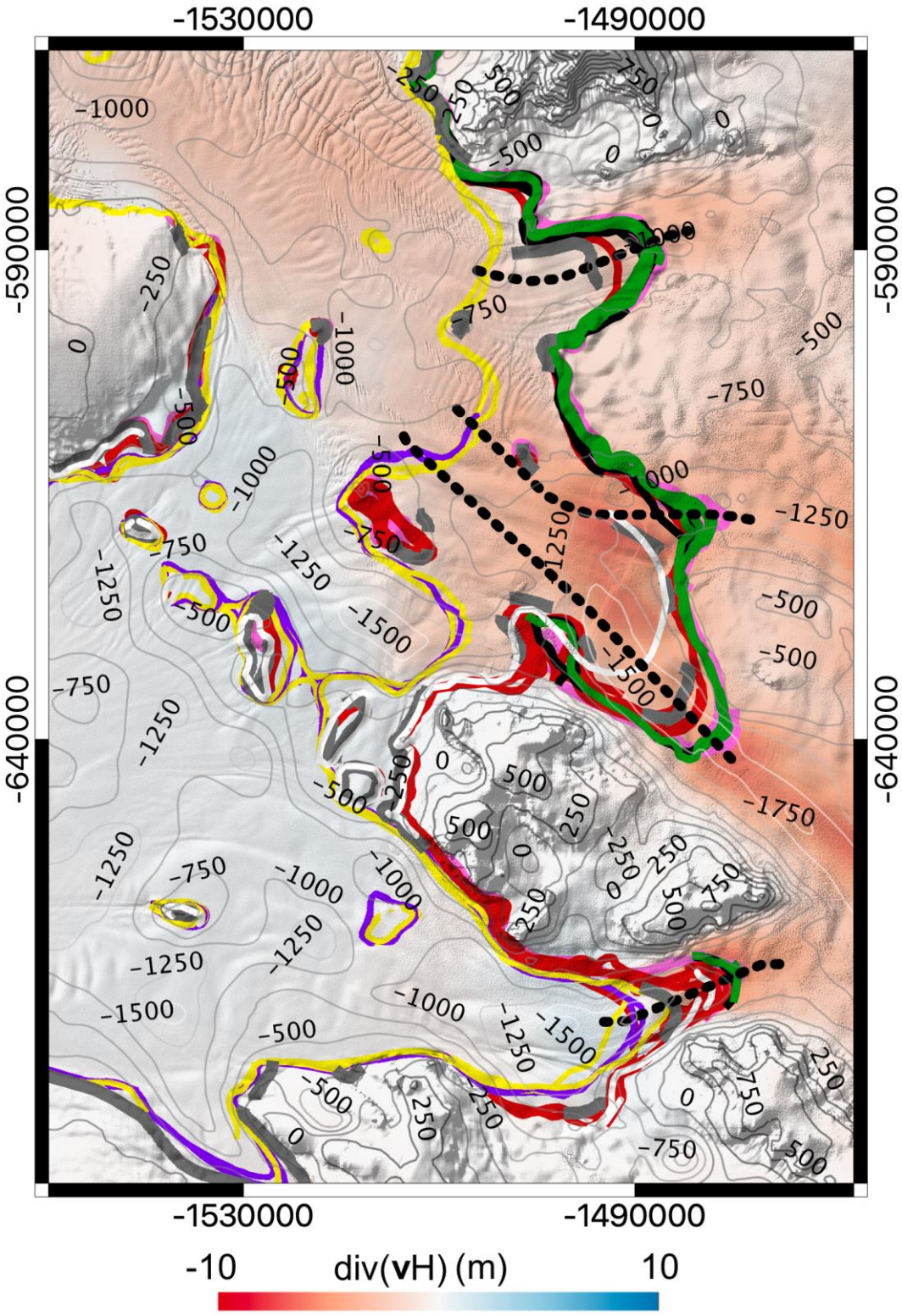

Figure S6. Divergence of the product of ice thickness and ice velocity. Thickness is from Bed Machine Antarctica version 2020_06_18. Velocity is from MEaSUREs products generated using Sentinel-1a/b speckle tracking data related for the time period 2018-2019. 500-m contour levels indicating bed elevation (grey)

Table S1. Maximum tidal height for the DInSAR data used in this study. Tidal values are shown in meters. The date format is Year/Month/Day/Hour/Minutes/Seconds.

CATS model	LatRef:	-74.46	LonRef:	-106.16					
Primary 1	**Secondary 1**	**Primary 2**	**Secondary 1**	**Tide Pr. 1**	**Tide Sec. 1**	**Tide Pr. 2**	**Tide Sec. 2**	**Δ Tide**	**h max**
19951106145736	19960115145736	19960115145736	19960219145736	-0.18	-0.27	-0.27	-0.21	0.15	-0.18
19951107145736	19951108145736	19960116145736	19960220145736	-0.16	-0.3	-0.3	-0.14	0.3	-0.14
20110406145826	20110412145826	20110418145826	20110415145826	0.16	0.15	-0.28	0.16	0.44	0.16
20141123050837	20141205050837	20141205050837	20141217050837	0.7	0.7	0.7	0.38	-0.31	0.7
20160210200332	20160211200332	20160313200332	20160314200332	-0.15	-0.08	0.12	0.03	-0.15	0.12
20160226200332	20160227200332	20160313200332	20160314200332	0.01	0.07	0.12	0.03	-0.14	0.12
20160313200332	20160314200332	20160430200332	20160501200332	0.12	0.03	0.07	-0.08	-0.07	0.12
20160313200332	20160314200332	20160329200332	20160330200332	0.12	0.03	0.31	0.27	0.04	0.31
20160329200332	20160330200332	20160430200332	20160501200332	0.31	0.27	0.07	-0.08	-0.11	0.31
20161206185030	20161207185030	20170123185030	20170124185030	-0.16	-0.17	-0.24	-0.31	-0.06	-0.16
20161221200332	20161222200332	20170122200332	20170123200332	-0.24	-0.2	-0.17	-0.24	-0.12	-0.17
20170515185030	20170516185030	20170531185030	20170601185030	0.47	0.41	0.12	0.14	0.08	0.47
20170920185115	20170921185115	20171022185115	20171023185115	0.27	0.1	-0.28	-0.27	0.18	0.27
20171022185030	20171023185030	20171123185030	20171124185030	-0.28	-0.27	-0.25	-0.16	0.08	-0.16
20171123185030	20171124185030	20180110185030	20180111185030	-0.25	-0.16	-0.1	-0.15	-0.13	-0.1
20180603185030	20180604185030	20180619185030	20180620185030	0.42	0.36	0.07	0.11	0.1	0.42
20180806185030	20180807185030	20180907185030	20180908185030	0.3	0.49	0.76	0.76	-0.18	0.76
20181112210330	20181113210330	20181128210330	20181129210330	-0.64	-0.57	-0.65	-0.58	0	-0.57
20200709185030	20200710185030	20200826185030	20200827185030	0.3	0.24	0.28	0.5	0.28	0.5
20200810185115	20200811185115	20200911185115	20200912185115	0.22	0.27	0.31	0.39	0.03	0.39
20200826185030	20200827185030	20201013185030	20201014185030	0.28	0.5	0.32	0.34	-0.2	0.5
20201116210330	20201117210330	20201218210330	20201219210330	-0.64	-0.73	-0.7	-0.63	0.16	-0.63
20201116210330	20201117210330	20201202210330	20201203210330	-0.64	-0.73	-0.71	-0.72	0.09	-0.64

Table S2. Inverse barometer effect (IBE) corrections related to the interferograms used in this study. IBE values are shown in meters whereas the date format is Year/Month/Day/Hour/Minutes/Seconds. h_{max}+IBE shows the maximum value used for this correction.

Primary 1	Secondary 1	Primary 2	Secondary 1	IBE Pr. 1	IBE Sec. 1	IBE Pr. 2	IBE Sec. 2	Δ IBE	h max + IBE
19951106145736	19960115145736	19960115145736	19960219145736	0.2459	0.2782	0.4111	0.1987	-0.2447	0.11
19951107145736	19951108145736	19960116145736	19960220145736	0.1171	-0.0067	0.2174	0.2212	0.1276	0.38
20110406145826	20110412145826	20110418145826	20110415145826	0.2074	0.3094	0.3094	0.3005	-0.1109	1.01
20141123050837	20141205050837	20141205050837	20141217050837	0.3259	0.3377	0.3151	0.2722	-0.0547	0.44
20160210200332	20160211200332	20160313200332	20160314200332	0.2349	0.2542	0.3151	0.2722	-0.0622	0.44
20160226200332	20160227200332	20160313200332	20160314200332	0.3151	0.2722	0.0664	0.1627	0.1392	0.44
20160313200332	20160314200332	20160430200332	20160501200332	0.3151	0.2722	0.2887	0.3405	0.0947	0.61
20160313200332	20160314200332	20160329200332	20160330200332	0.2887	0.3405	0.0664	0.1627	0.0445	0.61
20160329200332	20160330200332	20160430200332	20160501200332	0.1606	0.1761	0.2151	0.1431	-0.0875	0.01
20161206185030	20161207185030	20170123185030	20170124185030	0.1239	0.1131	0.3129	0.2151	-0.087	0.14
20161221200332	20161222200332	20170122200332	20170123200332	0.3883	0.3756	0.3908	0.4423	0.0642	0.86
20170515185030	20170516185030	20170531185030	20170601185030	0.3926	0.3256	0.2185	0.2239	0.0724	0.66
20170920185115	20170921185115	20171022185115	20171023185115	0.2185	0.2239	0.3623	0.3998	0.0321	0.24
20171022185030	20171023185030	20171123185030	20171124185030	0.3623	0.3998	0.3423	0.305	-0.0748	0.24
20171123185030	20171124185030	20180110185030	20180111185030	0.2861	0.2361	0.1528	0.104	0.0012	0.71
20180603185030	20180604185030	20180619185030	20180620185030	0.2856	0.2126	0.5735	0.4478	-0.0527	1.33
20180806185030	20180807185030	20180907185030	20180908185030	0.528	0.4592	0.2984	0.4053	0.1757	-0.11
20181112210330	20181113210330	20181128210330	20181129210330	0.5354	0.4648	0.2967	0.4074	0.1813	-0.1
20200709185030	20200710185030	20200826185030	20200827185030	0.1174	0.1122	0.0848	0.0485	-0.0311	0.55
20200810185115	20200811185115	20200911185115	20200912185115	0.1923	0.0582	0.3014	0.26	0.0927	0.65
20200826185030	20200827185030	20201013185030	20201014185030	0.0848	0.0485	0.3626	0.3358	0.0095	0.68
20201116210330	20201117210330	20201218210330	20201219210330	0.3242	0.3282	0.3473	0.5221	0.1708	-0.11
20201116210330	20201117210330	20201202210330	20201203210330	0.3242	0.3282	0.3905	0.4052	0.0107	-0.31